Journal of Drug Targeting

ISSN: 1061-186X (Print) 1029-2330 (Online) Journal homepage: http://www.tandfonline.com/loi/idrt20

Drug delivery to tumors using a novel 5-FU derivative encapsulated into lipid nanocapsules

Giovanna Lollo, Kevin Matha, Martina Bocchiardo, Jérôme Bejaud, Ilaria Marigo, Angelique Virgone-Carlotta, Thomas Dehoux, Charlotte Rivière, Jean Paul Rieu, Stephanie Briançon, Thomas Perrier, Olivier Meyer & Jean-Pierre Benoit

To cite this article: Giovanna Lollo, Kevin Matha, Martina Bocchiardo, Jérôme Bejaud, Ilaria Marigo, Angelique Virgone-Carlotta, Thomas Dehoux, Charlotte Rivière, Jean Paul Rieu, Stephanie Briançon, Thomas Perrier, Olivier Meyer & Jean-Pierre Benoit (2018): Drug delivery to tumors using a novel 5-FU derivative encapsulated into lipid nanocapsules, Journal of Drug Targeting, DOI: 10.1080/1061186X.2018.1547733

To link to this article: https://doi.org/10.1080/1061186X.2018.1547733

Accepted author version posted online: 21 Nov 2018.

Drug delivery to tumors using a novel 5-FU derivative encapsulated into lipid nanocapsules

Giovanna Lollo[1,2*], Kevin Matha[2,3*], Martina Bocchiardo[2], Jérôme Bejaud[2], Ilaria Marigo[4], Angelique Virgone-Carlotta[5], Thomas Dehoux[5], Rivière Charlotte[5], Rieu Jean Paul[5], Stephanie Briançon[1],Thomas Perrier[6], Olivier Meyer[6], and Jean-Pierre Benoit[2,3]

1, Université de Lyon, Université Claude Bernard Lyon 1, CNRS UMR 5007, Laboratoire d'Automatique et de Génie des Procédés (LAGEP), 43 bd 11 Novembre, 69622 Villeurbanne, France; Institut des Sciences Pharmaceutiques et Biologiques, 8 av Rockefeller, 69373 Lyon, France.

2, MINT, Université d'Angers, INSERM U1066, CNRS UMR 6021, Angers 49933, France.

3, Pharmacy Department, Angers University Hospital, 4 rue Larrey, Angers 49933, France

4, Veneto Institute of Oncology IOV-IRCCS, 35128 Padova, Italy

5, Univ Lyon, Université Claude Bernard Lyon 1, CNRS, Institut Lumière Matière, Villeurbanne, France

6, Carlina Technologies, 22 rue Roger Amsler, 49100 Angers, France

*Both authors equally contributed to the work

Abstract

In this work, a novel lipophilic 5-FU derivative was synthetized and encapsulated into lipid nanocapsules (LNC). 5-FU was modified with lauric acid to give a lipophilic mono-lauroyl-derivative (5-FU-C12, MW of about 342 g/mol, yield of reaction 70%). 5-FU-C12 obtained was efficiently encapsulated into LNC (encapsulation efficiency above 90%) without altering the physico-chemical characteristics of LNC. The encapsulation of 5-FU-C12 led to an increased stability of the drug when in contact with plasma being the drug detectable until 3h following incubation. Cytotoxicity assay carried out using MTS on 2D cell culture showed that 5-FU-C12-loaded LNC had an enhanced cytotoxic effect on glioma (9L) and human colorectal (HTC-116) cancer cell line in comparison with 5-FU or 5-FU-C12. Then, HCT-116 tumor spheroids were cultivated and the reduction of spheroid volume was measured following treatment with drug-loaded LNC and drugs alone. Similar reduction on spheroids volume was observed following the treatment with drug-loaded LNC, 5-FU-C12 and 5-FU alone, while blank LNC displayed a reduction in cell viability only at high concentration. Globally, our data suggest that the encapsulation increased the activity of the 5-FU-C12. However, in depth evaluations of LNC permeability into spheroids are needed to disclose the potential of these nanosystems for cancer treatment.

1. Introduction

5-Fluorouracil (5-FU, 5-fluoro-1H-pyrimidine-2,4-dione) is an antineoplasic agent used against a wide range of solid tumors (such as breast, head and neck, colon, pancreas and stomach tumors) [1]. In addition to its direct cytotoxic effect on tumor cells, the administration of low doses of 5-FU is able to induce a selective depletion of immunosuppressive myeloid cell population, namely myeloid-derived suppressor cells (MDSCs), which hampers tumor growth by enhancing antitumor T-cell response [2, 3].

Intracellularly 5-FU is converted into different cytotoxic metabolites (fluorodeoxyuridine monophosphate (FdUMP), fluorodeoxyuridine triphosphate (FdUTP) and fluorouridine triphosphate (FUTP). These active metabolites disrupt RNA synthesis and inhibit the action of thymidylate synthase (TS). The rate-limiting enzyme in 5-FU catabolism is dihydropyrimidine dehydrogenase (DPD), which converts 5-FU to its inactive metabolite dihydrofluorouracil (DHFU). More than 80% of administered 5-FU is normally catabolized primarily in the liver, where DPD is abundantly expressed, and as a consequence lower amounts of drug are able to reach the tumor target site [1]. Moreover, lacks in drug efficiency are caused by a non-favorable pharmacokinetic profile (i.e. poor distribution to the tumor tissue, short plasma half-life (15-20 min), rapid catabolism, schedule-dependent toxicity profile) and phenomenon of drug resistance (accelerated efflux of the active form by P-gp protein at the surface of cells, variation in DPD activity or gene amplification of TS) that occur frequently [4]. Additionally, 10–20% of patients treated with standard 5-FU usually show severe toxicities. DPD deficiency, a pharmacogenetic syndrome leading to limited detoxification capabilities, makes patients overexposed and prone to toxicities, thus often hampering treatment completion, when not directly life-threatening [5].

In this respect, to improve toxicity/efficacy balance [6], numerous modifications of the 5-FU structure have been performed and novel derivatives of 5-FU have been reported [7, 8]. Among them, tegafur, carmofur and floxuridine, 5-FU prodrugs, have proven their clinical efficacy with low toxicity and enhanced metabolic stability [9]. Also, capecitabine (Xeloda®), an oral fluoropyrimidine carbamate, that is activated selectively by the thymidine phosphorylase (TP) to form 5-FU, has been developed to increase tumor selectivity [10]. However, the results obtained using these derivatives are still marginal and 5-FU biodistribution and toxicity remain a challenging issue in oncology.

Strategies based on nano and micro medicines appear as a novel therapeutic approach to optimize drug biodistribution and antitumor effect [11-13]. The final aim is to design systems with a high drug loading and an optimal release of chemotherapeutic agents into the tumor tissue, which reduce drug accumulation and toxicity in healthy tissues [14, 15]. A liposomal formulation named LipoFufol® made of 5-FU combined to 2'-deoxyinosine and folic acid to improve its efficacy-toxicity balance has been developed [16]. Besides, solid lipid nanoparticles or PLGA nanoparticles have also

been described for targeted delivery of 5-FU [17, 18]. Even if the encapsulation in nanosystems results in an increased therapeutic efficacy of the drug, its high hydrophilicity represents a limiting step for the loading of such nanosystems as well as for the premature release of 5-FU from the nanocarriers when injected in blood.

In the present work, we combined the synthesis of a novel lipophilic 5-FU derivative made of 5-FU conjugated to lauric acid and a nanotechnology approach based on lipid nanocapsules (LNC). The rationale behind this strategy is that, increasing the lipophilicity of the drug, it will be possible to obtain a higher drug loading and a better controlled release of the drug once encapsulated into the lipid nanocarriers. The feasibility and transposability of the system were evaluated and the batch formulation was scaled up 20-fold. *In vitro* studies on glioma (9L) and colon (HCT-116) cancer cell lines to assess the efficacy of the derivative both in its free form or encapsulated into LNC were performed. Besides, three-dimensional (3D) spheroids made of HCT-116 cells were generated and the effect of 5-FU derivative alone and loaded into LNC was studied.

Globally, the approach presented in this paper was focused on the development of a novel 5-FU derivative-loaded LNC and on the development of a more predictive *in vitro* models to highlight the added value of nano-therapeutic strategies.

1. Materials and Methods

1.1 Chemicals

5-Fluorouracil (5-FU), formaldehyde, 4-dimethylaminopyridine (DMAP), *N*,*N*′ dicyclohexylcarbodiimide (DCC) and lauric acid were purchased from Sigma-Aldrich (St. Quentin-Fallavier, France). Acetonitrile, methanol and ethyl acetate were purchased from Fisher Scientific (Illkirch, France) and silica gel from Merck (Fontenay-sous-Bois, France). Labrafac® (glyceryl tricaprylate), Span 80® (sorbitane monooleate) and Kolliphor® HS 15 (polyethyleneglycol mono-and di-esters of 12-hydroxystearic acid and about 30% polyethylene glycol) were obtained from Abitec Corp. (Colombus, Ohio, USA), Fluka-Sigma-Aldrich and BASF (Ludwigshafen, Germany), respectively; NaCl was purchased from Prolabo (Fontenay-sous-Bois, France) and water was obtained from a MilliQ system (Millipore, Paris, France).

1.2 Synthesis and characterization of 5-FU-C12 derivative

1.2.1 Synthesis of 5-FU-C12

The synthetic procedure for the preparation of 5-FU-C12 (5-fluoro-2,4-dioxo-3,4-dihydropyrimidine-1(2H)-yl)methyl hexadecanoate) involved two steps and was performed according to the scheme below (Figure 1).

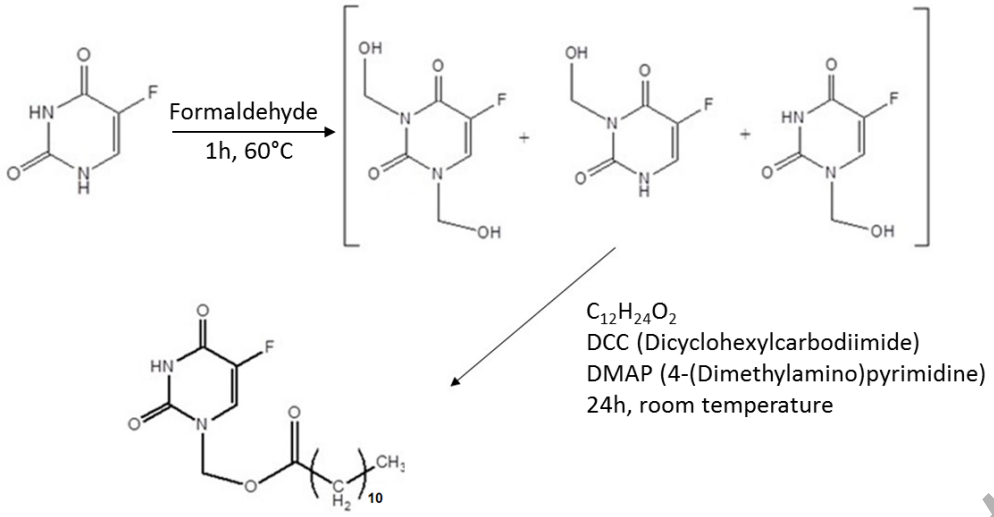

Figure 1: Scheme of 5-FU-C12 synthesis

Briefly, 5-FU (500 mg, 3.8 mmol) reacted with formaldehyde (37% wt.) in aqueous solution (50:50 v/v; 2.5 mL of formaldehyde/2.5 mL of MilliQ water (Millipore, Paris, France)) in a round-bottom flask immersed in a water bath (60 °C). The reaction was conducted under magnetic stirring for 1 h and gave as products a mixture of N-1-hydroxymethyl-5-fluorouracil, N-3-hydroxymethyl-5-fluorouracil and N,N'-1,3-bis(hydroxymethyl-5-fluorouracil) [19, 20].

Then, the round-bottom flask was cooled in an ice-bath (0-5 °C) and acetonitrile was added (15 mL). After, DCC (1.27 g, 6.08 mmol), DMAP (34 mg, 0.266 mmol) and lauric acid (1.23 g, 6.14 mmol) were added to achieve the esterification. The reaction mixture was stirred for 1 h at 0 °C, then 24 h at room temperature and monitored by thin-layer chromatography. The secondary product dicyclohexyl urea (DCU) was separated by filtration and eliminated after several washings with acetonitrile. The product was recovered by solvent evaporation under reduced pressure and purification on a silica gel chromatographic column (isocratic elution; eluent: dichloromethane/ethyl acetate 95:5 v/v).

1.2.2 Characterization of 5-FU-C12: ^{1}H NMR

Confirmation of the structure and purity of 5-FU-C12 were performed by ^{1}H NMR. NMR spectra were obtained on a Bruker 500 MHz spectrometer (Bruker France SAS, Wissembourg, France) using deuterated dimethyl sulfoxide (DMSO-d6) as solvent.

1.2.3 Pre-formulation studies: solubility of 5-FU-C12 derivative

The saturation solubility of the 5-FU-C12 derivative in different oils or solvents was determined by adding an excess amount of drug in 1 mL of various liquids in small vials. Vials were placed at room temperature or in a water bath at 60°C during 3h, and continuously stirred to reach equilibrium (48

h at 25°C). After that, drug mixtures were centrifuged at 1,700 g for 20 min at 20 °C (Centrifuge Eppendorf 5810R, Montesson, Paris, France). The supernatant was separated and added to acetonitrile and solubility was quantified by HPLC at 215 nm. The solubility studies were carried out in triplicate and results were reported as mean ± SD. LogP was also calculated through the program ACD/ChemSketch (Advanced Chemistry Development (ACD/Labs), Strasbourg, France).

1.2.4 HPLC determination of 5-FU-C12

Chromatography was performed using a Waters 717 Plus Autosampler and a Waters 600 Pump Controller (Waters S.A., Saint-Quentin-en-Yvelynes, France) with an XTerra® C18-RP18 5µm 150 mm x 4.6 mm column (Waters, Milford, Ireland) with precolumn and a Waters 2487 Dual Absorbance Photodiode Array Detector set at λ = 263 nm. A 40 µL aliquot of each filtrate was injected in duplicate into the HPLC column. The column was eluted at 1 mL/min flow rate using a gradient obtained by mixing amounts of MilliQ water (A) and acetonitrile (B). The initial mobile-phase composition was 90% A and 10% B; a first linear gradient was applied to reach a composition of 70% A 30% B after 5 min, a second linear gradient was applied to reach a composition of 100% B after 10 min, maintained for 5 min and then returned to 90% A and 10% B. The peak of 5-FU-C12 appears at 16.5 min. Data acquisition, analysis and reporting were performed using Empower chromatography software (Milford, Massachusetts, USA).

1.3 Development and characterization of blank and 5-FU-C12 loaded LNC

1.3.1 Preparation of blank and 5-FU-C12-loaded LNC

LNC were formulated using a phase inversion-based process previously described [21, 22]. Briefly, different amounts of 5-FU-C12 were firstly stirred in a mixture of Labrafac® and Span® 80. Then, 0.967 g of Kolliphor® were added together with NaCl (45 mg) and water (1.02 mL). Three temperature cycles (between 45 and 70 °C) were performed to obtain the phase inversion of the emulsion. Between these temperatures, there was a phase inversion zone (PIZ) at around 55-60 °C. At 1-3 °C from the beginning of the PIZ of the last temperature cycle, a rapid cooling and dilution with purified ice cooled water (2.15 g) led to LNC formation. The nanocapsules were then stored at 4 °C. Sterile 5-FU-C12 LNC batches were obtained by filtration through 0.22 µm Millipore® Stericup™ filter units (Merck, Darmstadt, Germany). Sterility of the formulation was assessed using soybean casein digest medium at 20-25°C and thioglycolate medium at 30-35°C incubated during 14 days and 5 days of subculture according to the European Pharmacopoeia (Ph Eur), 9 Ed (Confarma, Hombourg, France). Endotoxin content was assessed using chromogenic kinetic method with kinetic QCL Limulus Amebocyte Lysate in GMP conditions (Confarma, Hombourg, France).

1.3.2 Physico-chemical characterization

Particle size and ζ potential of colloidal systems were determined using a Zetasizer Nano ZS (Malvern Instruments, Worcestershire, UK). For size measurement, samples were diluted to an appropriate concentration in deionized water and each analysis was carried out at 25ºC with a detection angle of 173º. The ζ potential values were calculated from the mean electrophoretic mobility values, as determined by Laser Doppler Anemometry (LDA). For LDA measurements, samples were diluted in in 0.1mM KCl.

1.3.3 Cryogenic-transmission electron microscopy (cryoTEM)

To evaluate the morphology of blank and loaded LNC, diluted samples were dropped onto 300 Mesh holey carbon films (Quantifoil R2/1) and quench-frozen in liquid ethane using a cryo-plunge workstation (made at Laboratoire de Physique des Solides-LPS Orsay, France). The specimens were then mounted on a precooled Gatan 626 specimen holder, transferred in the microscope (Phillips CM120) and observed at an accelerating voltage of 120 kV (Centre Technologique des Microstructures (CTμ), platform of the University Claude Bernard Lyon 1, Villeurbanne, France).

1.3.4 Determination of drug encapsulation efficiency

Firstly, the mixtures of Labrafac® and Span®80, in which 5-FU-C12 was solubilized, were collected and analyzed by HPLC (after dilution 1:1000 in acetonitrile) to calculate the total amount of 5-FU-C12 dissolved. Once the LNC were formulated, they were filtered through a 0.22 µm filter to eliminate the free drug. Samples of drug-loaded LNC were prepared by dissolving an aliquot of LNC dispersion in acetonitrile (dilution 1:200) and 40 µL were injected in the HPLC according to the protocol previously described. The encapsulation efficiency (%) was determined according to the following formula:

$$EE\ (\%) = \frac{measured\ drug\ payload}{theoretical\ drug\ payload} \times 100$$

Linear titration curves, with freshly made 5-FU-C12 acetonitrile solutions at a concentration range from 0.5 to 25 µg/mL, were used to extrapolate results (r^2>0.999).

1.3.5 Storage stability studies in colloidal suspension of 5-FU-C12-loaded LNC

The stability of 5-FU-C12-loaded LNC was evaluated after storage at +4 °C during 1 month. The macroscopic aspect, particle size, polydispersity and leakage of the drug were assessed at fixed time intervals and after filtration using a Minisart® 0.22 µm filter (Merck, Fontenay-sous-Bois,

France). In addition, particle stability was also assessed following incubation during 48 h at 37°C with cell culture medium.

1.3.6 Stability study in plasma of 5-FU-C12-loaded LNC

The stability in a relevant physiological medium was evaluated using human plasma provided by Etablissement Français du Sang (EFS, Pays de la Loire, Nantes, France).

Samples of plasma were defrosted and diluted (80:20) with filtered PBS (0.22 µm filter). Thirty samples were prepared mixing 50 µL of 5-FU-C12-loaded LNC or 5-FU-C12 acetone solution and kept at 37°C in a water bath. At different time points (0, 5, 10, 15, 30, 60, 180, 360 min and 24 and 48 h), samples were taken and diluted with 800 µL of acetonitrile in order to precipitate plasma proteins and centrifuged at 12,290 g during 15 min at 4°C. Supernatants were recovered, filtered through 0.22 µm filter and analyzed by HPLC as previously described. Calibration curve of 5-FU-C12 in plasma from 1 to 22.5 µg/mL was performed (r^2>0.999).

1.3.7 *In vitro* release studies of 5-FU-C12-loaded LNC

The release rate of 5-FU-C12 from the loaded LNC was determined using an *in vitro* dialysis technique [23]. Briefly, a known suspension of 5-FU-C12-loaded LNC was dispersed in a solution of freshly prepared phosphate buffered saline (PBS), pH 7.4, containing Tween® 80 (0.1%, w/v). The mixture was incubated at 37°C and subjected to continuous shaking at 100 rpm, using magnetic stirring. The released 5-FU-C12 was sampled at defined time periods (0.5h, 1h, 3h, 5h, 8h, 12h, 24h and 48h). An aliquot was recovered and immediately replaced with an equal volume of fresh solution. The concentration of the aliquot was measured using the HPLC method previously described.

1.4 Scale-up formulation study

Batches of 5-FU-C12-loaded LNC were scaled up to 112 g (twenty times bigger than the lab scale). The experimental conditions were adapted in order to prepare up to 100 mL of LNC in a single step process. An intermediate volume (50 mL, 56g) was used in order to evaluate the robustness of the formulation process. Blank and 5-FU-C12-loaded LNC were characterized in terms of mean size, zeta potential, and encapsulation efficiency using the methods previously described.

1.5 *In vitro* experiments

1.5.1 Cell culture

Two cell lines have been cultured to carry out the experiments: rat 9L gliosarcoma cells and human HCT-116 colorectal carcinoma cancer cell.

9L cells were obtained from the European 127 Collection of Cell Culture (Sigma, Saint-Quentin Fallavier, France). HCT-116 colorectal carcinoma (CCL247) cell line was purchased from the American Type Culture Collection (ATCC, Manassas, Virginia, USA).

9L cells were grown in EMEM (Lonza, Verviers, Belgium) supplemented with 10% fetal bovine serum (Lonza), 1% antibiotics (10,000 units penicillin, 10 mg streptomycin, 25 µg amphotericin B/mL solubilized in appropriate citrate buffer (Sigma-Aldrich)) and 1% non-essential amino acids (Lonza).

HCT-116 line were cultured in DMEM-Glutamax (Lonza) supplemented with 10% of heat-inactivated fetal bovine serum (FBS; Sigma-Aldrich), 100 units/100 µg of penicillin/streptomycin. Cell lines (9L and HCT-116) were thawed and cultured in T75 flasks with filter caps (Thermo Scientific™ Nunc™, Villebon-sur-Yvette, France), maintained at 37 °C in a humidified atmosphere with 5% of CO_2.

1.5.2 *In vitro* cell viability

In vitro cytotoxicity assays were performed using CellTiter 96® AQueous One Solution cell proliferation assay kit (Promega, Charbonnières-Les-Bains, France) containing a tetrazolium compound (3-(4,5-dimethylthiazol-2-yl)-5-(3-carboxymethoxyphenyl)-2-(4-sulfophenyl)-2H-tetrazolium, inner salt; MTS). Briefly, 9L ($6{,}950\times10^3$ per well) and HT-116 cells ($3{,}500\times10^3$ per well) were plated into 96-well plates and incubated at 37°C during 48h in air controlled atmosphere (5% CO_2). The medium was removed and cells were treated during 24 or 48h with increasing concentrations 5-FU-C12 LNC diluted with serum free DMEM medium supplemented with 1% antibiotics (10,000 units penicillin, 10 mg streptomycin, 25 µg amphotericin B/mL solubilized in appropriate citrate buffer), 1% HEPES buffer, 1% NEAA (Non Essential Amino Acid) 100X (Lonza), 1% sodium pyruvate (Lonza), 1% N1 medium supplement 100X (0.5 mg/mL recombinant human insulin, 0.5 mg/mL, human transferrin partially iron-saturated, 0.5 µg/mL sodium selenite, 1.6 mg/mL putrescine, and 0.73 µg/mL progesterone (Sigma-Aldrich)). After incubation, cell survival percentage was determined using the CellTiter 96® AQueous One Solution cell proliferation assay kit. According to the procedure described by the supplier, medium with treatments was removed and 200 µL of a 1:5 diluted MTS solution were added in each well. After 2 h at 37 °C, the absorbance at 492 nm was recorded using a Microplater Reader (Multiskan Ascent®, Labsystem, Cergy Pontoise, France).

Cell viability (CV) percentage was evaluated through the following formula:

$$CV\ (\%) = \frac{Absorbance\ treated\ well}{Absorbance\ control\ well} \times 100$$

with Absorbance control well, the absorbance value of untreated cells (incubated only with fresh medium).

1.5.3 Dose response curves of *in vitro* cell viability data and IC50

Dose (concentration of drug treatments, µM) response (cellular viability, %) curves were plotted for the test after correction by subtracting the background (medium) absorbance. Percentage of viable cells was calculated based on the absorbance values (λ = 492 nm) in cells treated with media only (assumed as 100% viable). A linear model was used to estimate the regression parameters. In particular, the Log transformation of concentration used was calculated in order to have a normal distribution for this variable. This model allowed us to estimate the concentration of the drug required to reduce cell viability by 50% (IC50) and CI (confidence interval) stated at the 95% confidence level.

1.5.4 3D cell model: MCTS formation and treatment

Multi cellular tumor spheroids (MCTS) were formed according to a previous published method [24]. Briefly, MCTS were formed using HTC-116 cell line in Ultra Low Attachment (ULA) 96 wells Round-Bottom plate (Greiner bio-one) to avoid cell-substrate attachment. The cells were trypsinized and were counted using a Malassez grid in order to obtain 2,400 cells per milliliter. This concentration of cells (i.e., 480 cells per well in a volume of 200 µL) was chosen in order to obtain a single spheroid per well, with a spheroid diameter at the end of the experimentation not exceeding 500 µm.

The plate was centrifuged for 5 minutes at 1,200 g at room temperature to initiate the formation of spheroids. The plate was placed in the incubator under agitation at 37˚C and 5% CO_2 during the whole experiment. At the end of the first day after seeding, 100 µL of culture medium was added to ensure proper 3D growth. After two days after seeding, MCTS were treated with 5-FU aqueous solution, 5-FU-C12 diluted in acetone and 5-FU-C12-loaded LNC at various drug concentrations: 2, 10 and 50 µM. Blank LNC were also used to assess nonspecific toxicity that could arise from the system. MCTS were monitored at 24 and 48 h post treatment. Eight spheroids (n=8) were probed at each concentration. A ring of detaching cells appeared spontaneously after one day of treatment. The spheroids were transferred into new well plates to eliminate mechanically this uncohesive peripheral cell layer and to renew the drug and culture medium. Therefore, the reduction in volume that we monitor during treatment arises from a loss of viability as well as from a loss of cohesiveness.

1.6.5 Phase contrast follow up of MCTS volume

Photographs of MCTS were taken with an inverted microscope (Leica DMIRB) in phase contrast inside the 96-well plates at 0, 24 and 48h time points after 5-FU exposure. We performed edge detection using a sobel threshold for each spheroid using the Image J software. The resulting binary images were fitted to an ellipse of major (L_M) and minor (L_m) axes using the ImageJ "Analyse Particles" plugins. From this, a mean diameter was calculated, $D = (L_M + L_m)/2$. The volume V was then determined assuming that the spheroids are spherical $V = \pi D^3/6$.

1.6 Statistical analysis

For the results of *in vitro* cytotoxic activity evaluation, statistical differences were determined using non parametric tests, such as Wilcoxon-Mann-Whitney test and Kruskal-Wallis test. The type one error rate was taken as alpha = 5% ($p < 0.05$).

2. Results

2.1 Synthesis and characterization of 5-FU-C12 derivative

2.1.1 Synthesis of 5-FU-C12

In order to obtain the lipophilic 5-FU derivative named 5-FU-C12 made of 5-FU conjugated to lauric acid, a two-step process was performed. In the first step of the synthesis, pure 5-FU reacted with aqueous formaldehyde to give a mixture of *N*-*N1*-bis- (hydroxymethyl-5-fluorouracil) and mono-hydroxymethyl substituted 5-FU (*N*-1- hydroxymethyl-5-fluorouracil, *N*-3-hydroxymethyl-5-fluorouracil). As previously described by Liu *et al.*, [19] following this step, the 1H NMR spectrum showed that *N*-1-hydroxymethyl-5-fluorouracil was obtained in higher amount than the others [19]. Then, the preferential conjugation of lauric acid in the N1 position by means of DCC/DMAP chemistry was achieved. The alkyl chain was attached in preference to the functionalized nitrogen in position 1 because the amount of intermediate *N*-1-hydroxymethyl-5-fluorouracil was higher than the others [20] and also because this was the sterically less hindered and more nucleophilic site (due to its higher pKa value). After purification by silica gel column chromatography, 5-FU-C12 (molecular weight (MW) 342 g/mol) was recovered as the main product in the form of white powder with a yield of 70%.

2.1.2 Characterization of 5-FU-C12: 1H NMR

5-FU-C12 was characterized by 1H NMR analysis and the spectrum obtained is reported in Figure 2. 5-FU-C12 1H NMR spectrum clearly indicated that the peak at δ = 8.9 ppm was due to the aromatic -CH proton of 5-FU; peak at δ = 6.3 ppm was due to -CH2- of the bridging methylenic group

between 5-FU and lauric acid. Further, peaks at δ = 3.1, 2.3, 2.1 and 1.7 ppm may be assigned to the methylenic groups and terminal methyl group of the lauric acid chain.

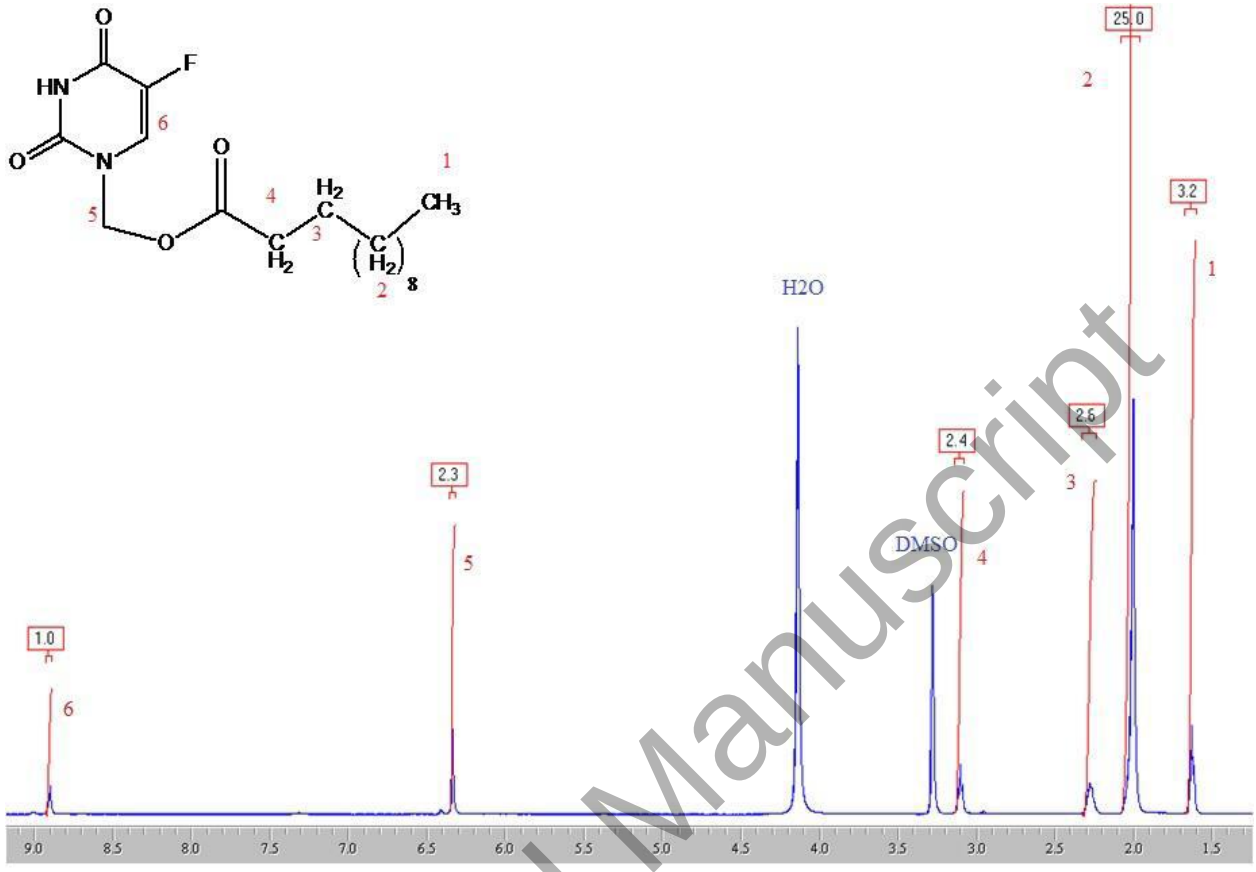

Figure 2: ^{1}H NMR spectrum of 5-FU-C12.

2.1.3 Pre-formulation: water solubility of 5-FU-C12

Water solubility of 5-FU-C12 was tested at two different temperature conditions (room temperature and 60°C) as showed in Table 1. The 5-FU derivative was practically insoluble in water as reported in Table 1. This finding confirmed the increased hydrophobic behavior of 5-FU-C12 compared to 5-FU, which is normally soluble in water (12 g/L, data from Ph Eur, 9 Ed).

Table 1: Solubility in water of 5-FU-C12 at different conditions (room temperature and 60°C).

Condition	Initial conc. 5-FU-C12 (mg/mL)	5-FU-C12 dissolved (%)	Solubility (mg/mL)	
Room Temperature	1.38	1.02	0.01	Practically insoluble
60 °C	1.50	5.62	0.09	

Subsequently, with the purpose of identifying the most adequate solubilizing agent for 5-FU-C12 to formulate 5-FU-C12-loaded LNC, we tested the solubility in different oils and organic solvents (ethanol and acetone) (see Table 2). In particular, we evaluated a series of excipients that are

generally used for the formulation of LNC [22, 25]. The solubility of 5-FU-C12 was also tested in the mixture of oil and surfactant (Labrafac® and Span® 80), currently used in other formulations to obtain loaded LNC [15]. Solubilization of 5-FU-C12 in oils was not possible after simple vortex passage (the unbundling of the bottom required a lot of time and was not effective). Samples were then maintained under magnetic stirring for 24 h, and plunged in a water bath set at 60 °C. After 48 h, samples were centrifuged and macroscopic observation did not reveal presence of sediment. Assays to assess the amount of solubilized product were performed using HPLC according to the method described in the experimental section. The results are shown in Table 2.

Table 2: Solubility of 5-FU-C12 in different oils (a) and class 3 solvents (b).

	Solubilizing agent	5-FU-C12 Solubility(mg/mL)
Class 3 solvent	Acetone	30.00
	Ethanol	3.81
Oil and surfactant	Labrafac®	14.21
	Captex® 8000	10.34
	Span® 80	13.60
	Mixture (Labrafac® + Span® 80)	15.05

As further proof of the increased lipophilic behavior of the derivative, we calculated the cLogP value : it was 4.48 for 5-FU-C12, while the value for 5-FU was -0.78.

2.2 Development and characterization of blank and 5-FU-loaded LNC

2.2.1 Physico-chemical characterization of blank and 5-FU-C12-loaded LNC

Blank and loaded LNC were obtained following the Phase Inversion Technique (PIT) previously described [15]. To load 5-FU-C12 into LNC, Labrafac® and Span® 80 were chosen for the first step of preparation (preliminary dissolution of the derivative before adding other components). The solubility of the active in the mixture of selected excipients (50/50 w/w) was confirmed using HPLC.

The results of the physico-chemical characterization of blank and 5-FU-C12-loaded LNC obtained with this process are showed on Table 3. The average size for all the systems developed was approximately 65 nm. The polydispersity index was below 0.1, indicating unimodal and narrow size distribution. The zeta potential values were neutral or slightly negative, ranging from -4 to -7 mV and corresponded to classical values obtained for LNC.

To evaluate the encapsulation efficiency of the drug into the LNC, samples of 5-FU-C12-loaded LNC were prepared and purified through 0.22 µm filtration prior to HPLC analysis. As indicated, the encapsulation efficiency at different payloads was high, around 98%. This result was due to the high hydrophobicity of the derivative, which was dissolved in the oily hydrophobic core of LNC. Finally, the endotoxin content was assessed and the value was under 5 EU/mL for every batch (data not

shown) according to the Ph Eur 9 and under GMP conditions. The value obtained for the endotoxin content was consistent with an IV administration of the LNC.

Table 3: Physico-chemical characterization of blank and 5-FU-C12-loaded LNC.

Formulation	5-FU-C12 payload* (mg/g)	Size* (nm)	PDI	ζ-potential* (mV)
Blank LNC	-	65 ± 3	<0.1	-6 ± 1
5-FU-C12-loaded LNC	1.7 ± 0.1	65 ± 2	<0.1	-4 ± 2
	2.4 ± 0.2	64 ± 3	<0.1	-2 ± 1
	4.5 ± 0.1	64 ± 1	<0.1	-4 ± 2

*Data represent average ± S.D.; PDI: polydispersity index, 5-FU-derivative payload = mg of 5-FU-derivative/g of LNC dispersion

A cryoTEM analysis of blank and 5-FU-C12-loaded LNC diluted twice in water, are shown in Figure 3. This observation was chosen in addition to the DLS technique because it allowed to discriminate the contribution of small versus big particles. Besides, DLS presented the size as a mean hydrodynamic radius and could therefore be biased by extreme sizes of nanoparticles [26]. Both LNC formulations presented almost monodispersed population with spherical shape and no differences were found between empty and loaded systems.

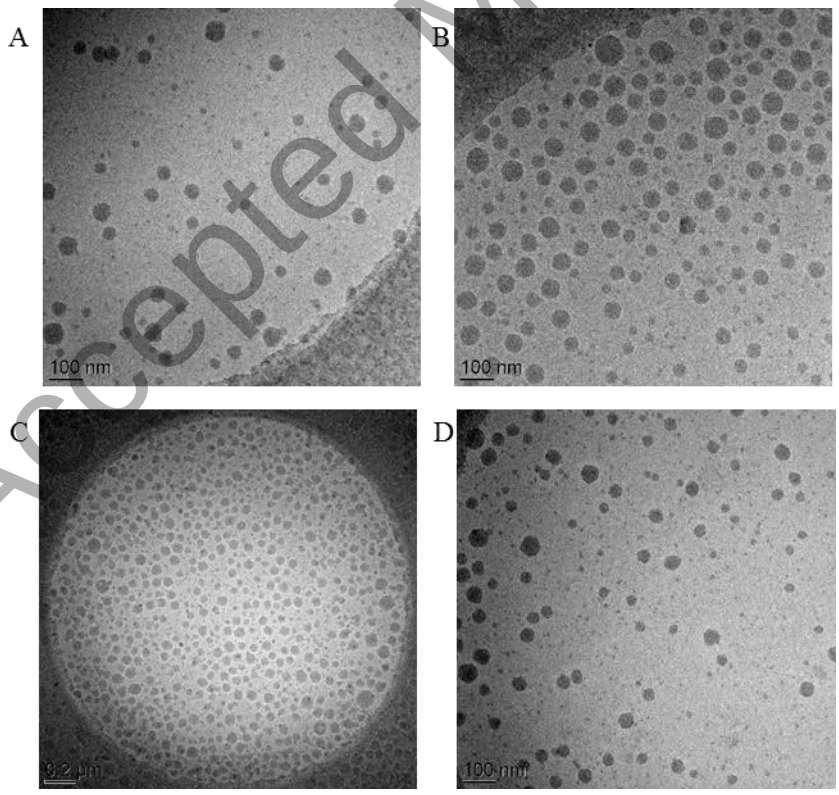

Figure 3: Microstructure obtained by cryoTEM of blank (A and B) and LNC loaded with 1.7 mg/g of 5-FU-C12 (C and D).

2.2.2 Storage stability in aqueous suspension

The different batches of 5-FU-C12-loaded LNC were stable over one month, indeed, no differences were observed in the average size, while a small increase in the PDI value, which remains below the value of 0.1, was observed after 1 month as shown in Figure 4.

Stability studies of the drug-loaded nanosystems were performed to evaluate the leakage of the derivative from the LNC at different payloads after 1 month of storage in water suspension (measurement of variation in the drug payload and, consequently, in the rate of encapsulation). No leakage of the derivative from the nanocapsules was detected over the period studied.

In addition, upon incubation in cell culture medium at 37°C during 48h, LNC still maintained their integrity in terms of size and polydispersity index.

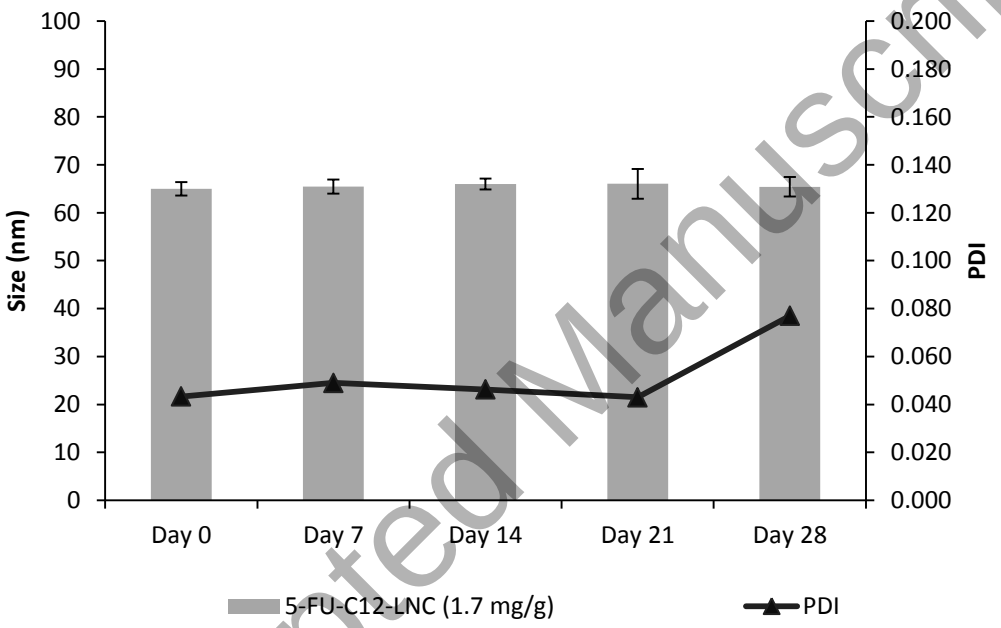

Figure 4: Size and PDI evolution over time of 5-FU-C12-loaded (1.7 mg/g) LNC in suspension at 4°C (n=3).

An *in vitro* release study to check the release of the drug from the nanocarriers, for the formulation with 5-FU-C12-loaded in the LNC, was carried out in PBS/Tween® 80. This experiment showed that 5-FU-C12 was not released from the LNC over 24h of incubation. Indeed, thanks to the hydrophobicity of the derivative, the drug was completely retained into the nanosystem.

2.2.3 Stability in plasma

Subsequently, the stability of encapsulated 5-FU derivative in LNC was investigated in human plasma by measuring with HPLC method the percentage of remaining intact drug over time. 5-FU-C12 acetone solution was also tested. As shown in Figure 5, the drug integrity of 5-FU-C12 was

maintained in its free form during the first 15 min, then the concentration decreased and only 50% of the drug was detected after 1h of incubation. In the case of encapsulated 5-FU-C12, almost 100 % of the drug was detected following 3h of incubation and 50% of the initial content was stable until 24 h of incubation. The improvement in drug stability detected at least during the first 3h of incubation was ascribed to LNC encapsulation which increased drug solubility and protect the drug from the rapid degradation.

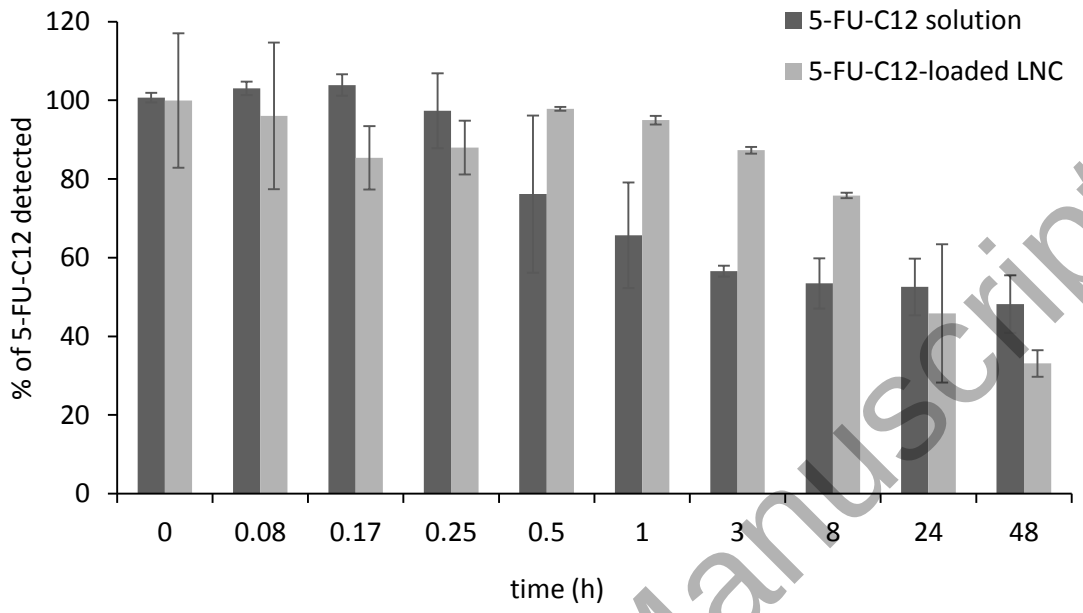

Figure 5: Stability of 5-FU-C12 following incubation of drug solution or encapsulated in LNC in human plasma.

2.3 Scale up of blank and 5-FU-C12 loadedLNC

In order to scale up the LNC formulation using the phase inversion method, two large volume batches were prepared in order to evaluate the robustness of the formulation process. Firstly, an intermediate batch corresponding to a batch ten times bigger than the laboratory one was produced. Then, a second batch twenty-fold bigger was obtained. The physico-chemical characteristics of both batches in terms of size, polydispersity index and zeta potential were assessed and the results of the characterization are reported in Table 4. No significant differences were found comparing the laboratory batch (scale x1) and the scale up batches (scale x10 corresponding to 56g of formulation and scale x20 corresponding to 112g of formulation). The LNC maintained their initial properties in terms of size and polydispersity indicating that the process was transposable to industrial settings.

Table 4: Physico-chemical characterization of blank LNC at different batch scales

	Scale x1 = 5.6g			Scale x10 = 56g			Scale x20 = 112g		
	Size (nm)	PDI	ζ-potential (mV)	Size (nm)	PDI	ζ-potential (mV)	Size (nm)	PDI	ζ-potential (mV)
1 month	65±2	<0.1	-	70±2	<0.1	-	70±2	<0.1	-10.2±2
2 months	73±3	<0.1	-6.68±2	66±2	<0.1	-5.84	73±2	<0.1	-

2.4 *In vitro* cell studies

2.4.1 *In vitro* cytotoxicity *on 2D cell growth*

In order to analyze the biological effect of the preparations, we tested the viability of glioma (9L) and colon cancer (HCT-116) cells following 24h and 48h of treatment with escalating doses of different formulations by using the MTS assay. 5-FU derivative in the free form (5-FU-C12 solubilized in acetone) or encapsulated into LNC compared to native 5-FU aqueous solution were tested. Blank LNC were also tested as control to exclude toxic effects of the nanocarriers. In the case of 9L cell line, cell viability was not affected upon 24h of incubation, therefore the effect following 48h of incubation was showed (Figure 6 A). While, HCT-116 cell viability was strongly reduced following 24h of exposure to treatments and no significant differences were observed upon 48h of incubation (Figure 6 B).

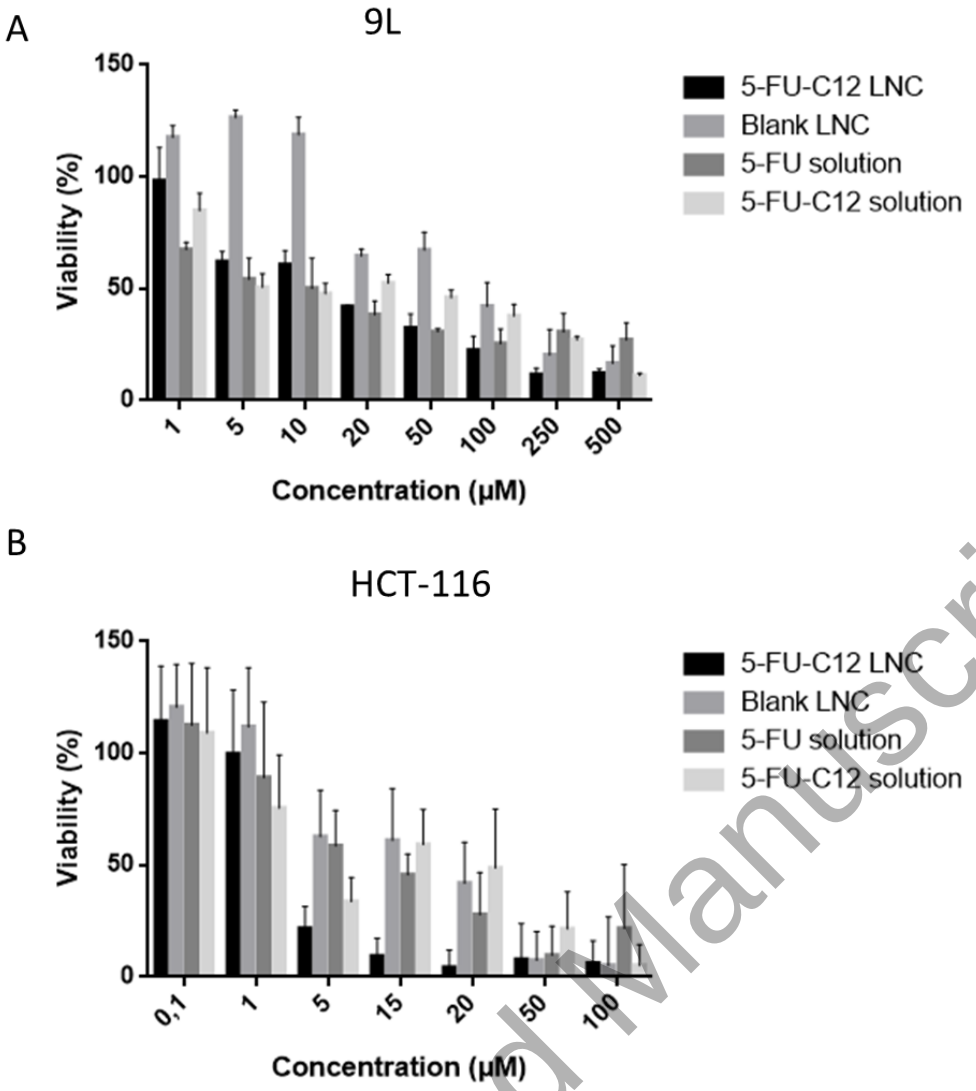

Figure 6: Cell viability of 9L (A) and HCT-116 (B) cells vs drug concentration after 48h incubation (37 °C) with blank and 5-FU-C12-loaded LNC, compared to free 5-FU (solution in water) and 5-FU-C12 (solution in acetone). Drug concentration is presented in log scale (n=5; mean ± S.D.).

After 48h of exposure to 5-FU-C12-loaded LNC, viability decreased as a function of the drug concentration exposure for both cell lines tested (Figure 6). IC50 values for drug (concentration µM) and LNC treatments (concentration mg/mL) and the respective confidence interval (µM or mg/mL), are shown in Table 5.

Table 5. IC50 (µM) and (mg/mL of LNC) of 5-FU-C12-loaded LNC compared to 5-FU-C12 derivative, 5-FU aqueous solution and blank LNC on 9L and HCT-116 cell line.

Formulation	IC50 (5-FU µM) and CI		IC50 (mg/mL LNC) and CI	
	9L	HCT-116	9L	HCT-116
Blank LNC	-	-	0.77 (0.53, 0.97)	0.193 (0.082, 0.457)
5-FU-C12 LNC	2.24 (1.75, 2.86)	2.48 (1.45, 4.22)	0.22 (0.17, 0.29)	0.058 (0.033, 0.098)
5-FU-C12 solution	16.91 (15.50, 22.88)	20.72 (11.20, 38.35)	-	-
5-FU water solution	9.09 (3.48, 23.78)	4.08 (1.056, 21.86)	-	-

A moderate cytotoxic effect on 9L cell line of 5-FU compared to 5-FU-C12 solution was found, the IC50 values being 9.09 and 16.91 µM, respectively. However, when the 5-FU-C12 was encapsulated into LNC, the cytotoxic effect was more pronounced with an IC50 value of 2.24 µM. Cytotoxicity on 9L cell line was observed for blank LNC (non-loaded nanocarrier dispersions diluted in culture medium at the same excipients concentration than that needed for loaded ones) only at high concentration around 0.77 mg/mL.

The viability of HCT-116 cells exposed to different concentrations of 5-FU alone or encapsulated into LNC was determined following 48 h of treatment. Pure 5-FU (water solution) was more effective than 5-FU-C12 solution being the values of IC50 of 4.8 and 20.72 µM, respectively. 5-FU-C12-loaded LNC showed a toxic effect more pronounced as compared with free drug being the IC50 value of 2.48 µM. Blank LNC were 3 times less toxic as compared to the loaded system being the values 0.193 and 0.053 mg/mL, respectively (Table 5).

2.4.2 *In vitro* cytotoxicity on 3D cell growth

To establish the impact on tumor viability of our formulations on a more lifelike *in vitro* culture system, we tested the dose response of 5-FU solution in comparison with the modified 5-FU-C12-loaded LNC during a 48 h treatment on a MultiCellular Tumor Spheroids (MCTS) derived from the HCT-116 cell line. The volume of MCTS was evaluated from phase contrast microscopy images as a readout of cytotoxic effect. The data reported in Figure 7 represent normalized MCTS volume for different drug treatments with respect to the control volume (MCTS not treated). Three different drug concentrations were tested: 2, 10 and 50 µM of 5-FU, 5-FU-C12 and 5-FU-C12 –loaded LNC.

As showed in the Figure 7, loaded-LNC with modified 5-FU-C12 and 5-FU-C12 or 5-FU in solution were able to reduce the volume of the spheroids after 2 days of treatment (D2) even at drug doses of 2 µM. The cytotoxic effect was more pronounced at higher doses (10 and 50 µM).

Similar to the non-specific toxicity observed in 2D cell culture, blank LNC induced a slight reduction of MCTS volume only at very high drug concentration.

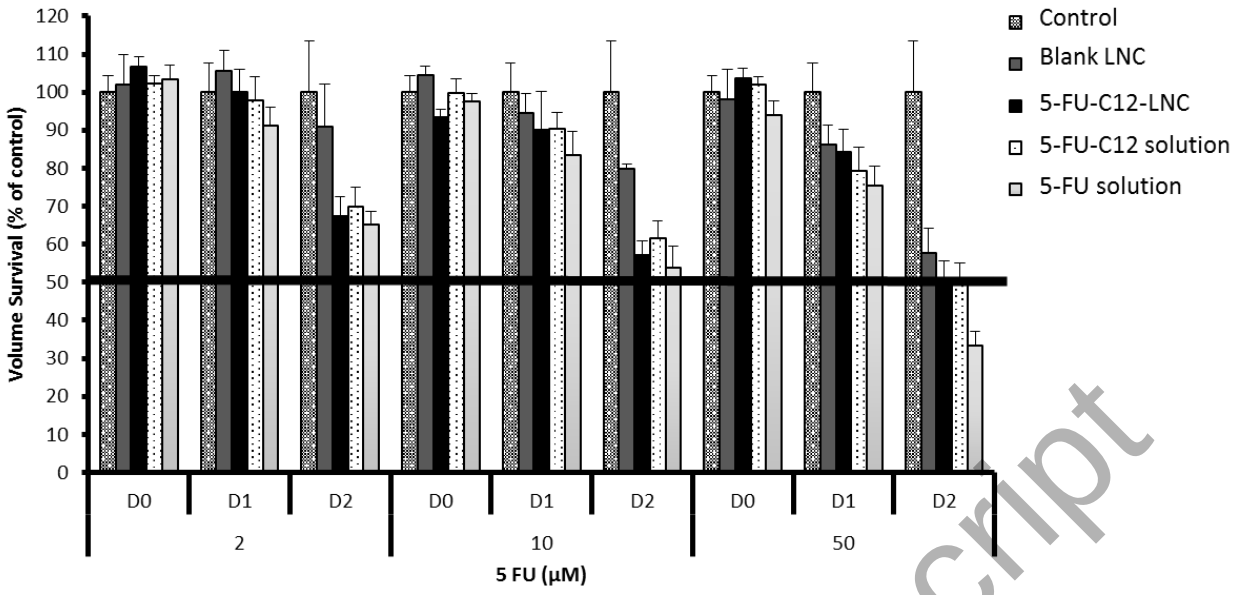

Figure 7: Normalized volume of multicellular HT116 spheroids after treatment with blank LNC, LNC loaded with 5-FU-C12, modified 5-FU-C12 dissolved in acetone and 5-FU clinical formulation. Spheroids were treated with different drug concentrations (2, 10 and 50 µM) at different time points (Day 0, Day 1 and Day 2).

3. Discussion

5-FU is a common chemotherapeutic agent used for the treatment of different cancers [27]. Its rapid catabolism, short half-life (15-20 min), indiscriminate biodistribution, aspecific cytotoxicity and myelosuppression impose the need to develop an alternative formulation and delivery system for this anticancer drug [27]. When administered intravenously, approximately 90% of an injected dose of 5-FU is metabolized to inactive 5-FUH2 by DPD in the liver, peripheral blood mononuclear cells, intestinal mucosa, pancreas, lungs and kidneys, thus limiting its efficacy. Thus, the maintenance of a therapeutic serum concentration requires continuous administration of high doses of this drug with subsequent severe toxic effects [6].To solve the limitations related with 5-FU administration, two main strategies have been investigated in the present work: i) the synthesis of a novel 5-FU derivative and ii) the encapsulation of this active into lipid nanocapsules. As compared to other lipid-based nanocarriers like liposomes, LNC display some convenient features; in fact, they are prepared by an organic solvent free and soft-energy procedure and present great storage stability [15]. In addition, physico-chemical properties of optimal LNC (i.e. size range, polydispersity index) can be monitored and designed *ad hoc*, since they are strongly dependent on

the proportions of different components (oily phase, hydrophilic surfactant, aqueous phase - water plus sodium chloride).

Different studies report attempts to improve the *in vivo* performances of 5-FU, through the development of prodrugs and encapsulation in drug delivery nanosystems [8, 16, 28]. However, the low encapsulation efficiency due to the inherent hydrophilic nature of 5-FU was observed for different nanocarriers [16]. In our work, 5-FU was modified with a biocompatible moiety, lauric acid, to obtain a lipid6drug conjugate having more affinity for the hydrophobic core of the LNC (production yield of 70%). The easy synthesis and higher degree of purification ensured the complete elimination of formaldehyde in the first step of the synthesis (Figure 1). 5-FU-C12 was characterized by nuclear magnetic resonance (NMR) and the ^{1}H NMR (Figure 2) indicates that only one chain of lauric acid was conjugated to the N1 position. Previously, a derivative of 5-FU named 5-FUDIPAL obtained by conjugating palmitic acid to the drug was published. In this compound, two lipid tails were attached to the lipid–5-FU conjugate (in N1 and N3 position) which imparted hydrophobic characteristics to 5-FU [23]. In our case, the conjugation of only a single chain of lauric acid to N1 position strongly affects the hydrophobicity of the novel compound, 5-FU-C12. Indeed, pre-formulation solubility studies carried out in a polar solvent (water), non-polar solvents (acetone and ethanol), oils and surfactants demonstrated that 5-FU-C12 was not soluble in water while freely soluble in polar solvents and oils. Its hydrophobicity makes 5-FU-C12 a suitable candidate for LNC encapsulation. In Figure 3, we demonstrated that LNC loaded with 5-FU derivative with a hydrodynamic size of around 65 nm and a neutral surface charge. Using the PIT method, spherical and monodispersed systems, also confirmed by cryoTEM images, were obtained. The conjugated lauric acid tail was expected to elevate the non-covalent interaction between the drug and the oily core of the system resulting in a high amount of drug loading and absence of fast release. Moreover, the encapsulation provides protection to the drug from plasmatic degradation. 5-FU-C12-loaded LNC were incubated with human plasma and the drug was detected until 3h following incubation, while 5-FU-C12 was eliminated earlier being detected only 1h following incubation (Figure 5). Considering that the plasmatic half-life of 5-FU is of around 30 min [29], the LNC here developed led to an important increase in drug detection when incubated with plasma.

The biological evaluation of 5-FU-C12 on 2D cell culture measured by MTS showed that 5-FU-C12-loaded LNC had an enhanced cytotoxic effect on 9L and HTC-116 cell line in comparison with modified drug alone, being the IC50 values eight and ten times lower compared to the 5-FU-12 alone. Also, loaded-LNC were more cytotoxic with respect to 5-FU. It was reported that following 48 h of treatment on HCT-116 cells, the IC50 value of PLGA nanoparticles loaded with 5-FUDIPAL, a similar palmitic acid-conjugate, was around 23 µM [23], twenty times higher in comparison to the IC50 value of 5-FU-C12-loaded LNC (IC50 around 2 µM). Besides, 5-FU-loaded pH-sensitive

liposomes having different lipid compositions had been also described and their activity tested on HCT-116 cell line. The authors found differences in cell sensitivity when treated with the formulation obtained and ascribed the differences and the resulting low anti-cancer activity of liposomes to the low entrapment efficiency of 5-FU [30]. Low encapsulation efficiency and premature release of the drug strongly affect the efficacy of the nanosystems encapsulating 5-FU in these nanosystems. Comparing the results on HCT-116 cell line to other nanosystems loaded with 5-FU derivative, the encapsulation into LNC was more effective in reducing cell viability. 5-FU-C12 loaded LNC here developed were able to encapsulate in a high amount the novel hydrophobic compound and to retain the drug in the oil core even when diluted in simulated physiological media, therefore promising to increase the half-life of the drug.

In a 2D cell model free drug or nanosystems had to enter into a cell monolayer to exert their cytotoxic activity. The difference in the cytotoxic effect is related to the stability, solubility, release and internalization ability of drug when entering cells. From our result is evident that the encapsulation of the 5-FU-C12 enhanced the stability and internalization of the drug, being the effect of drug loaded LNC more pronounced in comparison to free drug.

Once demonstrated the enhanced cytotoxic effect of drug loaded-LNC on 2D cell culture, HCT-116 cells were used to form 3D spheroids and the effect of 2 day-treatment, with 5-FU-C12 loaded LNC, 5-FU or 5-FU-C12 alone, was investigated. The aim was to test the LNC developed in a more complex system that mimics the 3D chemical and physical gradients that occur in *in vivo* tumors. The volume of the spheroids was measured as a readout for cytotoxicity after 24 and 48 h of treatment. As showed in Figure 7, for all the treatments we observed a reduction of MCTS volume as time increases, demonstrating the inhibition of MCTS growth. Interestingly, the effect of drugs alone and 5-FU-C12 loaded LNC had a similar effect on MCTS volume, suggesting a comparable efficacy in 3D systems. Moreover, the effect of blank LNC on MCTS growth is less pronounced than that of loaded LNC. This observation is particularly evident at day 2 at the highest concentration tested (0.875 mg/mL). This result contrasts with the observations made on the 2D cell model, where the non-specific toxicity of blank LNC appears at lower concentration (0.193 mg/mL). This difference should be analyzed considering that we used different readouts for the efficacy in 2D and 3D cell model [31]. In 2D we evaluated cell death through a metabolic essay (MTS) while in 3D we evaluated MCTS growth, which results from the equilibrium between cell death and proliferation. The difference we observe thus suggests that blank LNC causes cell death, which is the origin of their toxicity, but does not affect cell proliferation. In future works, there are many parameters that should be investigated to confirm this analysis, such as permeability of the spheroids to the treatment [32, 33].

Globally, from the preliminary results, we observed that the encapsulation into LNC does not hamper the penetration into the spheroid, and enhance cytotoxic effect respect to the other treatments. Further in depth studies taking into account permeability, distribution of the drug and mechanism of internalization of drug-loaded LNC into MCTS has to be performed to fully disclose the efficacy of this system.

4. Conclusion

In the present work, we reported evidence about the feasibility of an oily-core nanoformulation for 5-FU-derivative encapsulation. Using a simple synthesis process, we developed with a high yield of production a novel lipophilic 5-FU derivative namely 5-FU-C12, which was successfully encapsulated into LNC. The novel formulation obtained enhanced the solubility and the stability of the drug when in contact with plasma. Further, *in vitro* studies were carried out in different tumor cell lines (9L and HCT-116) to assess the cytotoxic activity of the encapsulated drug with respect to the drug in solution or the commercial one. 5-FU-C12-loaded LNC resulted in a higher cytotoxic effect compared with 5-FU-C12 alone or 5-FU while blank LNC showed cytotoxic ability only at very high concentrations indicating possible limited toxic effects of the carriers. Then, to obtain reliable and detailed information about LNC-tumor interaction in a more physiologic situation, we analyzed the effects of the treatments on HCT-116 3D-spheroid cultures. The results evidenced that the effect on spheroids survival was at least similar between drug-loaded LNC, 5-FU-C12 and 5-FU alone. We can therefore state that 5-FU-C12 encapsulation in a complex system does not reduce the penetration capacity into the spheroids. Further research will be needed to make these nanosystems not only comparable to solution treatments in their effect on 3D systems but to make them more effective.

Acknowledgments

Authors are thankful to Pierre-Yves Dugas from the Univ Lyon, Université Claude Bernard Lyon 1, CNRS, C2P2 UMR 5265, for his kind help and expertise for cryoTEM observation.

This work has been carried out within the research program of NICHE, financially supported by EuroNanoMed-II (4th call), RESOLVE, financially supported by EuroNanoMed-III (8th call) and ITMO Cancer within the frame of the Programme Plan Cancer 2014-2019 (no. PC201507).

Bibliography

1. Longley DB, Harkin DP, Johnston PG. 5-Fluorouracil: mechanisms of action and clinical strategies [Review Article]. Nature Reviews Cancer. 2003;3:330. doi: 10.1038/nrc1074.
2. Vincent J, Mignot G, Chalmin F, et al. 5-Fluorouracil Selectively Kills Tumor-Associated Myeloid-Derived Suppressor Cells Resulting in Enhanced T Cell–Dependent Antitumor Immunity. Cancer Research. 2010;70(8):3052-3061. doi: 10.1158/0008-5472.can-09-3690.
3. Ugel S, Delpozzo F, Desantis G, et al. Therapeutic targeting of myeloid-derived suppressor cells. Current Opinion in Pharmacology. 2009 2009/08/01/;9(4):470-481. doi: https://doi.org/10.1016/j.coph.2009.06.014.
4. Neto OV, Raymundo S, Franzoi MA, et al. DPD functional tests in plasma, fresh saliva and dried saliva samples as predictors of 5-fluorouracil exposure and occurrence of drug-related severe toxicity. Clinical Biochemistry. 2018 2018/04/04/. doi: https://doi.org/10.1016/j.clinbiochem.2018.04.001.
5. Yang CG, Ciccolini J, Blesius A, et al. DPD-based adaptive dosing of 5-FU in patients with head and neck cancer: impact on treatment efficacy and toxicity. Cancer Chemotherapy and Pharmacology. 2011 2011/01/01;67(1):49-56. doi: 10.1007/s00280-010-1282-4.
6. Lee JJ, Beumer JH, Chu E. Therapeutic drug monitoring of 5-fluorouracil. Cancer Chemotherapy and Pharmacology. 2016 2016/09/01;78(3):447-464. doi: 10.1007/s00280-016-3054-2.
7. S E Ward EK, J Cowan,M Marples, B Orr, and M T Seymour. The clinical and economic benefits of capecitabine and tegafur with uracil in metastatic colorectal cancer. Br J Cancer. 2006;3(95):1.
8. Álvarez P, Marchal JA, Boulaiz H, et al. 5-Fluorouracil derivatives: a patent review. Expert Opinion on Therapeutic Patents. 2012 2012/02/01;22(2):107-123. doi: 10.1517/13543776.2012.661413.
9. P Cellier BL, L Martin, B Vié, C Chevelle, V Vendrely, A Salemkour, C Carrie, G Calais, P Burtin, L Campion, M Boisdron-Celle, A Morel, V Berger, E Gamelin. Phase II study of preoperative radiation plus concurrent daily tegafur-uracil (UFT) with leucovorin for locally advanced rectal cancer. BMC Cancer. 2011;11:98.
10. Zhang M WW, Liu J, Yang H, Jiang Y, Tang W, Li Q, Liao X. Comparison of the effectiveness and toxicity of neoadjuvant chemotherapy regimens, capecitabine/epirubicin/cyclophosphamide vs 5-fluorouracil/epirubicin/cyclophosphamide, followed by adjuvant, capecitabine/docetaxel vs docetaxel, in patients with operable breast cancer. Onco Targets Ther. 2016 8(9):3443-50.
11. Henderson LA, Shankar LK. Clinical Translation of the National Institutes of Health's Investments in Nanodrug Products and Devices. The AAPS Journal. 2017 2017/03/01;19(2):343-359. doi: 10.1208/s12248-016-9995-x.
12. Grabbe S, Haas H, Diken M, et al. Translating nanoparticulate-personalized cancer vaccines into clinical applications: case study with RNA-lipoplexes for the treatment of melanoma. Nanomedicine. 2016;11(20):2723-2734. doi: 10.2217/nnm-2016-0275. PubMed PMID: 27700619.

13. Sykes EA, Dai Q, Sarsons CD, et al. Tailoring nanoparticle designs to target cancer based on tumor pathophysiology. Proceedings of the National Academy of Sciences. 2016;113(9):E1142-E1151. doi: 10.1073/pnas.1521265113.
14. Lollo G, Hervella P, Calvo P, et al. Enhanced in vivo therapeutic efficacy of plitidepsin-loaded nanocapsules decorated with a new poly-aminoacid-PEG derivative. International Journal of Pharmaceutics. 2015 2015/04/10/;483(1):212-219. doi: https://doi.org/10.1016/j.ijpharm.2015.02.028.
15. Sasso MS, Lollo G, Pitorre M, et al. Low dose gemcitabine-loaded lipid nanocapsules target monocytic myeloid-derived suppressor cells and potentiate cancer immunotherapy. Biomaterials. 2016 2016/07/01/;96:47-62. doi: https://doi.org/10.1016/j.biomaterials.2016.04.010.
16. Fanciullino R, Mollard S, Giacometti S, et al. In Vitro and In Vivo Evaluation of Lipofufol, a New Triple Stealth Liposomal Formulation of Modulated 5-Fu: Impact on Efficacy and Toxicity. Pharmaceutical Research. 2013 2013/05/01;30(5):1281-1290. doi: 10.1007/s11095-012-0967-2.
17. Roullin V-G, Deverre J-R, Lemaire L, et al. Anti-cancer drug diffusion within living rat brain tissue: an experimental study using [3H](6)-5-fluorouracil-loaded PLGA microspheres. European Journal of Pharmaceutics and Biopharmaceutics. 2002 2002/05/01/;53(3):293-299. doi: https://doi.org/10.1016/S0939-6411(02)00011-5.
18. Patel MN, Lakkadwala S, Majrad MS, et al. Characterization and Evaluation of 5-Fluorouracil-Loaded Solid Lipid Nanoparticles Prepared via a Temperature-Modulated Solidification Technique. AAPS PharmSciTech. 2014 2014/12/01;15(6):1498-1508. doi: 10.1208/s12249-014-0168-x.
19. Liu Z, Fullwood N, Rimmer S. Synthesis of allyloxycarbonyloxymethyl-5-fluorouracil and copolymerizations with -vinylpyrrolidinone [10.1039/B002092N]. Journal of Materials Chemistry. 2000;10(8):1771-1775. doi: 10.1039/b002092n.
20. Liu Z, Rimmer S. Synthesis and release of 5-fluorouracil from poly(N-vinylpyrrolidinone) bearing 5-fluorouracil derivatives. Journal of Controlled Release. 2002 2002/05/17/;81(1):91-99. doi: https://doi.org/10.1016/S0168-3659(02)00048-2.
21. B. Heurtault PS, B. Pech, J. E. Proust, and J. P. Benoit. A novel phase inversion - based process for the preparation of lipid nanocarrier. Pharm Res. 2002;19(6):875–880.
22. Moysan E, Gonzalez-Fernandez Y, Lautram N, et al. An innovative hydrogel of gemcitabine-loaded lipid nanocapsules: when the drug is a key player of the nanomedicine structure [10.1039/C3SM52781F]. Soft Matter. 2014;10(11):1767-1777. doi: 10.1039/c3sm52781f.
23. Ashwanikumar N, Kumar NA, Asha Nair S, et al. 5-Fluorouracil–lipid conjugate: Potential candidate for drug delivery through encapsulation in hydrophobic polyester-based nanoparticles. Acta Biomaterialia. 2014 2014/11/01/;10(11):4685-4694. doi: https://doi.org/10.1016/j.actbio.2014.07.032.
24. Virgone-Carlotta A, Lemasson M, Mertani HC, et al. In-depth phenotypic characterization of multicellular tumor spheroids: Effects of 5-Fluorouracil. PLOS ONE. 2017;12(11):e0188100. doi: 10.1371/journal.pone.0188100.
25. Lollo G, Vincent M, Ullio-Gamboa G, et al. Development of multifunctional lipid nanocapsules for the co-delivery of paclitaxel and CpG-ODN in the treatment of

glioblastoma. International Journal of Pharmaceutics. 2015 2015/11/30/;495(2):972-980. doi: https://doi.org/10.1016/j.ijpharm.2015.09.062.
26. Wibroe PP, Ahmadvand D, Oghabian MA, et al. An integrated assessment of morphology, size, and complement activation of the PEGylated liposomal doxorubicin products Doxil®, Caelyx®, DOXOrubicin, and SinaDoxosome. Journal of Controlled Release. 2016 2016/01/10/;221:1-8. doi: https://doi.org/10.1016/j.jconrel.2015.11.021.
27. Gusella M, Crepaldi G, Barile C, et al. Pharmacokinetic and demographic markers of 5-fluorouracil toxicity in 181 patients on adjuvant therapy for colorectal cancer. Annals of Oncology. 2006;17(11):1656-1660. doi: 10.1093/annonc/mdl284.
28. Carrillo E, Navarro SA, Ramírez A, et al. 5-Fluorouracil derivatives: a patent review (2012 – 2014). Expert Opinion on Therapeutic Patents. 2015 2015/10/03;25(10):1131-1144. doi: 10.1517/13543776.2015.1056736.
29. Bocci G, Danesi R, Di Paolo A, et al. Comparative Pharmacokinetic Analysis of 5-Fluorouracil and Its Major Metabolite 5-Fluoro-5,6-dihydrouracil after Conventional and Reduced Test Dose in Cancer Patients. Clinical Cancer Research. 2000;6(8):3032-3037.
30. Udofot O AK, Israel B, Agyare E. Cytotoxicity of 5-fluorouracil-loaded pH-sensitive liposomal nanoparticles in colorectal cancer cell lines. Integr Cancer Sci Ther. 2015;2(5):245-252.
31. Solomon MA, Lemera J, D'Souza GGM. Development of an in vitro tumor spheroid culture model amenable to high-throughput testing of potential anticancer nanotherapeutics. Journal of Liposome Research. 2016 2016/07/02;26(3):246-260. doi: 10.3109/08982104.2015.1105820.
32. Ho WY, Yeap SK, Ho CL, et al. Development of Multicellular Tumor Spheroid (MCTS) Culture from Breast Cancer Cell and a High Throughput Screening Method Using the MTT Assay. PLOS ONE. 2012;7(9):e44640. doi: 10.1371/journal.pone.0044640. PubMed PMID: PMC3435305.
33. Takechi-Haraya Y, Goda Y, Sakai-Kato K. Control of Liposomal Penetration into Three-Dimensional Multicellular Tumor Spheroids by Modulating Liposomal Membrane Rigidity. Molecular Pharmaceutics. 2017 2017/06/05;14(6):2158-2165. doi: 10.1021/acs.molpharmaceut.7b00051.